Effect of Block Structure on the Micellization and Gelation of Aqueous Solutions of Copolymers of Ethylene Oxide and Butylene Oxide

Zhuo Yang, Simon Pickard, Nan-Jie Deng, Raymond J. Barlow, David Attwood, and Colin Booth*

Manchester Polymer Centre, Departments of Chemistry and Pharmacy, University of Manchester, Manchester M13 9PL, U.K.

*Received August 27, 1993**

ABSTRACT: Oxyethylene/oxybutylene block copolymers $E_{41}B_8$, $E_{21}B_8E_{21}$, and $B_4E_{40}B_4$ were prepared by sequential anionic polymerization and characterized by gel permeation chromatography and NMR spectroscopy. Their association behavior in aqueous solution was investigated by surface tension and static and dynamic light scattering. The diblock copolymer $E_{41}B_8$ and the triblock copolymer $E_{21}B_8E_{21}$ associated by closed processes to form micelles, those of the diblock copolymer being much larger. The triblock copolymer $B_4E_{40}B_4$ associated by a process having characteristics of open association. A low-temperature clouding–clearing effect was noted for solutions of copolymer $E_{21}B_8E_{21}$. Thermally-reversible sol → gel → sol transitions were observed on heating or cooling concentrated solutions of diblock copolymer $E_{41}B_8$, but concentrated solutions of the two triblock copolymers did not gel.

Introduction

The micellization and gelation of diblock and triblock copolymers of ethylene oxide and butylene oxide (E_mB_n and $E_mB_nE_m$, where E represents an oxyethylene unit and B an oxybutylene unit) in aqueous solution have been reported in recent publications from this laboratory,[1-6] together with a brief study of drug release from gels formed from one of the systems.[3] Biomedical applications have provided a stimulus to much previous work (see, e.g., refs 7–9) on the micellization and gelation of aqueous solutions of triblock copolymers of ethylene oxide and propylene oxide ($E_mP_nE_m$, where P represents an oxypropylene unit). However, the association effects are interesting in their own right, as many recent publications testify (see, e.g., refs 10–15). Other than our own work, the studies have concentrated on $E_mP_nE_m$ copolymers, since these materials are commercially available. However, the use of oxyethylene–oxybutylene block copolymers avoids problems related to chain transfer which are inherent in the polymerization of propylene oxide.[16]

Direct comparison of the micellization and gelation properties of copolymers of identical overall composition and chain length but with different block structures has been largely neglected, possibly because of the lack of suitable materials. One systematic study of this type[17] concerned the association in aqueous solution of block copolymers related to the commercially-available $E_mP_nE_m$ copolymer L64 (BASF Pluronic or ICI Synperonic PE), a material containing 40 wt % E. In that work, triblock copolymer $E_{14}P_{30}E_{14}$ and the corresponding diblock copolymer, $E_{26}P_{29}$, were found to have almost identical association properties. However, copolymer L64 is not typical of the $E_mP_nE_m$ copolymers which excite current interest, since its association in solution at or near room temperature is very limited and its concentrated solutions do not gel. This behavior of copolymer L64 is consistent with a mechanism of gelation dominated by packing of well-developed micelles, with the gel–sol boundaries determined by micellar concentration and size.[3-6,11-15]

Considering systems in which the micelles have generally high association numbers, a comparison[4] of the behavior of E_mB_n and $E_mB_nE_m$ copolymers containing 60–90 wt % E suggested that a diblock copolymer would have a lower critical micelle concentration (cmc) compared with a triblock copolymer of the same overall composition and B block length. The present work was designed to investigate that result under more closely controlled conditions and to extend the study to include an "inverted" triblock copolymer, $B_mE_nB_m$. From previous investigations of diblock copolymers,[4-6] which included work on copolymers $E_{49}B_8$ and $E_{30}B_8$, it was known that a diblock copolymer of the approximate formula $E_{40}B_8$ would micellize and that its concentrated micellar solution would gel. The present paper describes the preparation and study of such a copolymer and the two corresponding triblock copolymers.

Experimental Section

The copolymers were prepared by sequential anionic polymerization of ethylene oxide and butylene oxide. All reagents were distilled and dried before use, and vacuum line and ampule techniques were used in order to minimize initiation by moisture at any stage. Initiator solutions were prepared by reacting freshly-cut potassium with an appropriate alcohol, diol or glycol, the ratio [OH]/[OK] being adjusted to ensure a controlled rate of polymerization. The methods have been described in detail previously:[1,4] those used for the three copolymers under discussion are summarized later in this paper. The prepared samples were characterized by gel permeation chromatography (GPC) and nuclear magnetic resonance spectroscopy (NMR): their molecular characteristics are summarized in Table 1.

The GPC system consisted of four μ-Styragel columns (Waters Associates, nominal porosities from 500 to 10^6 Å) eluted by tetrahydrofuran (THF) at room temperature and a flow rate of 1 cm^3 min^{-1}. Samples were dissolved in THF at a concentration of 2 g dm^{-3}, and their emergence was detected by differential refractometry (Waters Associates Model 410). Calibration was with a series of poly(oxyethylene) samples of known molar mass, and derived molar masses were as if poly(oxyethylene). Analysis of the GPC curve gave the molar mass at the peak (M_{pk}). The width of the peak, approximately corrected for instrumental spreading, gave an estimate of the ratio of mass-average to number-average molar mass (M_w/M_n).

^{13}C NMR spectroscopy was used to determine the average composition (i.e., mole fraction or weight fraction E) and the number-average molar mass. Polymer samples were dissolved in either $CDCl_3$ or C_6D_6 (0.1 g cm^{-3}), and spectra were obtained by means of a Varian Unity 500 spectrometer operated at 125.5

* Abstract published in *Advance ACS Abstracts*, March 15, 1994.

0024-9297/94/2227-2371$04.50/0

Table 1. Molecular Characteristics of the Block Copolymers

overall formula	M_n/(g mol^{-1}) (NMR)	M_w[a]/(g mol^{-1})	mol % E (NMR)	wt % E (NMR)
$E_{41}B_8$	2400	2640	84.5	76.0
$E_{21}B_8E_{21}$	2390	2630	84.2	76.5
$B_4E_{40}B_4$	2340	2460	82.9	74.8

[a] Based on M_n (from NMR) and $M_w/M_n \approx 1.05$–1.10 (from GPC).

MHz. Spectral assignments were taken from previous work.[18] In the polymerizations of butylene oxide, apart from "abnormal" additions to the initiator, it was found that all additions of butylene oxide were tail-to-head

$$-OCH_2CH(Et)OCH_2CH(Et)O^-)$$

and that all hydroxy end groups were secondary, with no evidence of unsaturation. Integrals of resonances associated with end and chain groups were used to obtain the chain length of the polymer prepared in the first stage of copolymerization, while those of the chain group (–OCH_2CH_2– or –OCH_2CH–) and the side group (–CH_2CH_3) were used to the obtain overall composition. A combination of these two quantities gave the overall molecular formula of the copolymer. To check the purity of the block copolymers, particularly the possible presence of homopolymers or copolymers initiated by moisture, the intensities of the end group resonances were compared with those of resonances associated with EB block junctions.

The short B blocks of copolymer $B_4E_{40}B_4$ and the segmented B block of copolymer $E_{21}B_8E_{21}$ (split in the center with a tail-to-tail placement) resulted in complicated patterns of resonances of the carbons of the B units. This "oligomer" effect, which did not affect the present analysis, will be discussed elsewhere.[19]

$E_{41}B_8$. The polymerization of butylene oxide (10.28 g) was initiated by 2-butanol, partly in the form of its potassium salt (ratio [OH]/[OK] ≈ 13; 0.0205 mol of alcohol plus salt). Polymerization was carried out at 40 °C for 3 days and then at 75 °C for 7 days, i.e., until polymerization was complete, as judged by the absence of condensable monomer. A small sample of the polymer gave M_{pk} = 558 g mol^{-1} and $M_w/M_n \approx 1.1$ (from GPC) and 7.6 B units including the end groups (from NMR). The NMR result corresponded to M_n = 547 g mol^{-1}, compared with M_n = 576 g mol^{-1} expected. The integrals of the resonances of carbons of the hydroxy end groups were sightly larger than those of carbons of the initiator residues, possibly because of a small proportion of difunctional chains (B_{14}, <2 mol %), though this result was within an absolute uncertainty of ±2% originating in the signal-to-noise ratio of the spectra.

The bulk of the poly(oxybutylene) (10.70 g) was used to initiate the polymerization of ethylene oxide (32.61 g). For safety, and to avoid crystallization of the product, polymerization was carried out starting at room temperature but progressing to 70 °C over a period of 1 week, until conversion was complete. The resulting copolymer had M_{pk} = 2690 g mol^{-1} and $M_w/M_n \approx 1.1$ (from GPC) and 84.5 mol % E (from NMR), corresponding to an E block length of 41.4 units. Overall NMR gave M_n = 2400 g mol^{-1} and 76.0 wt % E compared with M_n = 2340 g mol^{-1} and 75.3 wt % E expected. The integrals of resonances of carbons of end groups and junction groups were identical. In accordance with these results, the copolymer was denoted $E_{41}B_8$. Considering the uncertainty of the NMR analysis, possible impurities, present in very small amounts, were triblock copolymer $E_{41}B_{14}E_{41}$, originating from difunctional poly(oxybutylene), and poly(oxyethylene) E_{82}, originating from moisture introduced in the second stage.

$E_{21}B_8E_{21}$. The polymerization of butylene oxice (14.78 g) was initiated by 1,2-butanediol partly in the form of its potassium salt (ratio [OH]/[OK] ≈ 8; 0.0304 mol of diol plus salt). Polymerization was carried out at 50 °C for 3 days and then at 75 °C for 7 days. A small sample of the polymer gave M_{pk} = 563 g mol^{-1} and $M_w/M_n \approx 1.03$ (from GPC) and 7.8 B units including the end groups (from NMR), corresponding to M_n = 562 g mol^{-1} compared with M_n = 576 g mol^{-1} expected. The integrals of the resonances of carbons of the hydroxy end groups were identical with those originating from carbons of the tail-to-tail addition to the initiator (–OCH(Et)CH_2OCH_2CH(Et)–).

The bulk of the poly(oxybutylene) (12.09 g) was used to initiate the polymerization of ethylene oxide (36.85 g). The polymerization was carried out starting at room temperature and progressing to 70 °C over a period of 1 week. The resulting copolymer had M_{pk} = 2890 g mol^{-1} and $M_w/M_n \approx 1.1$ (GPC) and 84.2 mol % E (NMR), corresponding to 41.6 E units. Overall, NMR gave M_n = 2390 g mol^{-1} and 76.5 wt % E, compared with M_n = 2340 g mol^{-1} and 75.3 wt % E expected. The integrals of resonances of carbons of end groups, which were all primary OH, and those of EB junction groups were identical. In accordance with these results, the copolymer was denoted $E_{21}B_8E_{21}$. Considering the uncertainty of the NMR analysis, a possible impurity, present in a very small amount, is poly(oxyethylene) E_{42}, originating from moisture introduced at the second stage.

$B_4E_{40}B_4$. The polymerization of ethylene oxide (29.99 g) was initiated by diethylene glycol [α-hydroxy-ω-hydroxybis(oxyethylene)] partly in the form of its potassium salt (ratio [OH]/[OK] ≈ 10.0; 0.0196 mol of glycol plus salt). Polymerization was started at 35 °C and increased to 60 °C (in order to prevent crystallization) until completion after 8 days. A small sample of the polymer gave M_{pk} = 1840 g mol^{-1} and $M_w/M_n \approx 1.1$ (from GPC) and 39.8 E units including end groups (from NMR), corresponding to M_n = 1750 g mol^{-1} compared with M_n = 1760 g mol^{-1} expected.

The bulk of the polymer(oxyethylene) (30.36 g) was used to initiate the polymerization of butylene oxide (9.96 g). Polymerization at 55–60 °C was complete after 5 days. The resulting copolymer had M_{pk} = 2660 g mol^{-1} and $M_w/M_n \approx 1.05$ (GPC) and 17.1 mol % B (NMR), corresponding to 8.2 B units split between two blocks. Overall, NMR gave M_n = 2340 g mol^{-1} and 74.8 wt % E, compared with M_n = 2340 g mol^{-1} and 75.3 wt % E expected. The integrals of resonances of carbons of end groups, which were all secondary OH, were marginally larger than those of carbons of EB junction groups but still within the estimated uncertainty of ±2 mol %. In accordance with these results, the copolymer was denoted $B_4E_{40}B_4$. A possible impurity, present in a very small amount, was poly(oxybutylene) B_8, originating from moisture introduced at the second stage.

Purification. The copolymers were purified either by precipitation from dilute solution in dichloromethane by adding hexane or by equilibration of the copolymer with warm hexane before cooling to 10 °C and retaining the concentrated phase. If necessary, the purification procedure was repeated, the criterion used being the observation of a single micellar peak in dynamic light scattering (see later in this paper).

Clouding. Aqueous solutions of the copolymers in small test tubes were slowly heated (0.5 K min^{-1}) in a water bath to 100 °C, and clouding (if any) was observed visually. Further observations of clouding were made by light scattering, as described below.

Surface Tension. Surface tensions (γ) of dilute aqueous solutions were measured by detachment of a Wilhelmy plate. The glass plate was a microscope cover slip with the surface roughened by mild etching. The usual precautions were taken to ensure cleanliness, and the water was double-distilled and filtered (Millipore Millex-GS, triton-free, 0.22 μm). The plate was suspended from a Beckman LM-600 microbalance which was calibrated with standard weights. Solutions were held at the temperature of measurement (40 ± 0.5 °C) by means of a thermostated water jacket. The force of detachment was measured after 10 min and at intervals thereafter until consistent readings were obtained. The accuracy of measurement was checked by frequent determination of γ of water (69.5 ± 0.3 mN m^{-1}; expected at 40 °C, 69.6 mN m^{-1}).

Light Scattering. Solutions for light scattering were generally clarified by filtering through Millipore filters (Millex-GS, three times through a 0.22-μm-porosity filter and one or more times through a 0.1-μm-porosity filter), with the final filtration being directly into the cleaned scattering cell. The refractive index increment was determined by means of an Abbé 60/ED precision refractometer (Bellingham and Stanley).

Static light scattering intensity measurements were made by means of a Malvern PCS100 instrument with vertically polarized incident light of wavelength 488 nm supplied by an argon ion laser (Coherent Innova 90) operated at 500 mW or less. The intensity scale was calibrated against benzene. Measurements

were made at angles of 45°, 90°, and 135° to the incident beam. In an experiment, measurements were made either on solutions at a given temperature over a range of concentration or on solutions of given concentration over a range of temperature. In the latter case, the temperature of the scattering cell was raised or lowered at *ca.* 1 K min^{-1}.

The temperature dependence of the intensity of scattered light was also determined by means of a modified Sofica instrument with unpolarized light of wavelength 633 nm supplied by a 5-mW stabilized helium–neon laser (Uniphase Model 1122). For purposes of comparison with results obtained using the other instrument, scattering intensities were calibrated against scattering from benzene by measuring scattering from toluene acting as a secondary standard.

Dynamic light scattering measurements were made by means of the Malvern instrument described above combined with a Malvern K7027 autocorrelator using 60 linearly-spaced channels with a far-point delay of 1024 sample times. Measurements of scattered light were made at an angle of 90° to the incident beam. The data were analyzed either by the CONTIN method,[20] thus gaining information on the distribution of decay rates, or, if appropriate, by a single-exponential fit of the correlation curve.

Gelation. The gel–sol behavior of concentrated aqueous solutions of the diblock copolymers was investigated as follows. A solution of the block copolymer was enclosed in a small tube and observed on heating from −15 to 80 °C, and the change from a mobile to an immobile system (or vice versa) was determined by inverting the tube. The method served to define the sol–gel transition temperatures to about ±1 K.

Results and Discussion

Clouding. The clouding temperature of a 1 wt % solution of copolymer $B_4E_{40}B_4$, observed visually, was $T_c \approx 60$ °C, whereas a 1 wt % solution of copolymer $E_{41}B_8$ remained clear up to the limit of the test (95 °C). Similar clouding behavior was recorded for 5 wt % solutions. The relatively low clouding temperature of copolymer $B_4E_{40}B_4$, compared to that of the diblock copolymer, correlates with its unusual association properties: see later in this paper.

Solutions of copolymer $E_{21}B_8E_{21}$ of similar concentration were found to cloud at low temperatures and then to clear. For example, a 1 wt % solution prepared at low temperature (*ca.* 10 °C) clouded at 23 °C and cleared at 34 °C, remaining clear up to 95 °C. This effect is described in more detail later.

Dynamic Light Scattering. Various solutions in the concentration range 4–100 g dm^{-3} and temperature range 30–80 °C were studied by dynamic light scattering. The results were analyzed by the constrained regularization CONTIN technique developed by Provencher[20] and were used primarily to confirm the occurrence of association and determine the distribution of decay rates, hence the distribution of apparent diffusion coefficients (D_{app}) and, by application of the Stokes–Einstein equation, the distribution of apparent hydrodynamic radii ($r_{h,app}$, radius of the hydrodynamically-equivalent hard sphere corresponding to D_{app}): i.e., by use of

$$r_{h,app} = kT/(6\pi\eta D_{app}) \quad (1)$$

where k is Boltzmann's constant and η is the viscosity of water at temperature T. Given the sampling time used in the experiments, i.e., 5 μs, the minimum hydrodynamic radius detectable was $r_{h,app} \approx 1.2$ nm.

Examples of intensity distributions of $\log(r_{h,app})$ obtained for solutions of the copolymers at 50 °C are shown in Figure 1. The intensity distributions found for copolymers $E_{21}B_8E_{21}$ and $E_{41}B_8$ were narrow, as expected for closed micellization, whereas the distribution found for copolymer $B_4E_{40}B_4$ was wide, indicating a wide range of particle size. As concentration was increased, the narrow intensity distribution widened slightly (see results for copolymer $E_{41}B_8$ in Figure 1), but this relatively small effect did not explain the difference in properties between solutions of copolymers $E_{21}B_8E_{21}$ and $E_{41}B_8$, on the one hand, and those of copolymer $B_4E_{40}B_4$ on the other.

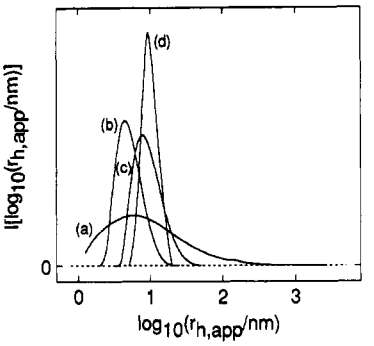

Figure 1. Dynamic light scattering from aqueous solutions of block copolymers at 50 °C. Normalized intensity distributions of the logarithm of the apparent hydrodynamic radius obtained for: (a) $B_4E_{40}B_4$, c = 60 g dm^{-3}; (b) $E_{21}B_8E_{21}$, c = 60 g dm^{-3}; (c) $E_{41}B_8$, c = 20 g dm^{-3}; (d) $E_{41}B_8$, c = 4 g dm^{-3}.

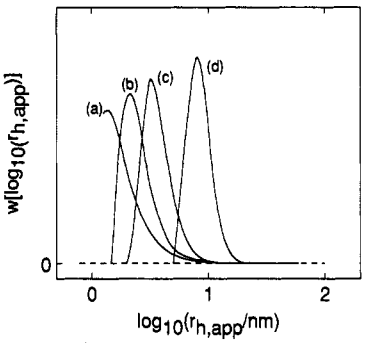

Figure 2. Dynamic light scattering from aqueous solutions of block copolymers at 50 °C. Normalized weight distributions of the logarithm of the apparent hydrodynamic radius obtained for: (a) $B_4E_{40}B_4$, c = 60 g dm^{-3}; (b) $B_4E_{40}B_4$, c = 100 g dm^{-3}; (c) $E_{21}B_8E_{21}$, c = 60 g dm^{-3}; (d) $E_{41}B_8$, c = 20 g dm^{-3}.

Assuming that intensities are proportional to wM, and hence to $wr_{h,app}^3$, the intensity distributions were transformed to "weight" distributions of particle size as shown in Figure 2. This representation illustrates very well the increase in $r_{h,app}$ of associated species along the series: $B_4E_{40}B_4 < E_{21}B_8E_{21} < E_{41}B_8$. It is evident that high concentrations are needed to achieve even limited association of copolymer $B_4E_{40}B_4$ in solutions at 50 °C.

The clear difference in the association behavior of copolymer $B_4E_{40}B_4$ compared to those of the other two copolymers can be illustrated in another way. The natural logarithm of the field correlation function for delay time τ, in the form $\ln[\beta^{1/2}g^{(1)}(\tau)]$, where β is the spatial coherence factor, is plotted against delay time in Figure 3. The data points for copolymers $E_{21}B_8E_{21}$ and $E_{41}B_8$ fall onto straight lines, as expected for narrow distributions of decay rates (hence narrow distributions of diffusion coefficients and particle size). By contrast, the data points for copolymer $B_4E_{40}B_4$ fall onto a curve, indicating a wide distribution of decay rates for this system, symptomatic of a wide distribution of particle size.

Concentration dependences of the average values of D_{app} were not systematically determined. For the one case investigated, intensity-average values of $1/r_{h,app}$ for micelles of copolymer $E_{41}B_8$ at 30 °C were extrapolated to zero concentration to obtain the z-average inverse radius $(1/r_h)_z^{-1}$: see Figure 4 and Table 2. Weight-averages, $(1/r_{h,app})^{-1}$, given in Table 2 for all copolymers, were derived from the decay rate distributions obtained for solutions

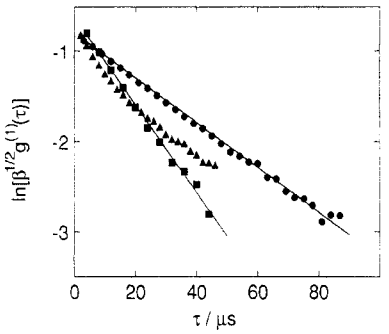

Figure 3. Dynamic light scattering from aqueous solutions of block copolymers. Natural logarithm of the field correlation function, $\ln[\beta^{1/2}g^{(1)}(\tau)]$, versus delay time τ for: (●) $E_{41}B_8$, c = 37 g dm^{-3}, T = 30 °C; (■) $E_{21}B_8E_{21}$, c = 60 g dm^{-3}, T = 50 °C; (▲) $B_4E_{40}B_4$, c = 60 g dm^{-3}, T = 50 °C. β is the spatial coherence factor.

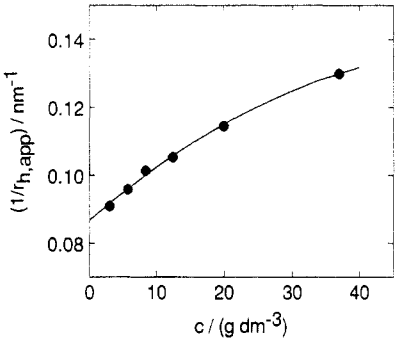

Figure 4. Dynamic light scattering from aqueous solutions of block copolymer $E_{41}B_8$ at 30 °C. Inverse apparent hydrodynamic radius versus copolymer concentration.

Table 2. Association of Block Copolymer in Aqueous Solution[a]

copolymer	T/°C	$r_{h,app}$[b]/nm	r_h[c]/nm	M_w/(10^4 g mol^{-1})	N_w	r_t/nm
$E_{41}B_8$	20			11.1	42	5.2
	25			13.2	50	5.6
	30		11.5	16.1	61	6.0
	35	10		20.6	78	6.5
	50					
$E_{21}B_8E_{21}$	35	1.5		1.2	4.6	1.9
	50	3.5		1.5	5.8	2.2
$B_4E_{40}B_4$	50	1.9				

[a] Estimated uncertainties: r_t, M_w, and N_w, ±10%; r_h, ±1 nm. [b] Weight-average value, $(1/r_{h,app})_w^{-1}$, estimated by the CONTIN method from results for moderately concentrated solutions (20–60 g dm^{-3}). [c] z-average value, $(1/r_h)_z^{-1}$, obtained by extrapolation of $(1/r_{h,app})_z^{-1}$ to zero concentration; see Figure 4.

of moderate concentrations *via* the CONTIN method. Those listed for copolymers $E_{21}B_8E_{21}$ and $B_4E_{40}B_4$ are near to the lower limit of detection and are less accurate on that account. Assuming that the positive concentration dependence of $1/r_{h,app}$ found for micelles of copolymer $E_{41}B_8$ (see Figure 4) holds for all associated species in solution, the values of $r_{h,app}$ serve as approximate lower limits to the true values.

Critical Concentrations from Surface Tension. Plots of surface tension (γ) of solutions at 40 °C against log c (c = concentration) are illustrated in Figure 5. Equilibrium readings were obtained within 1 h. The plots for solutions of copolymers $E_{41}B_8$ and $E_{21}B_8E_{21}$ are relatively straighforward, with identifiable critical concentrations (c_{cr} = 0.3 ± 0.1 and c_{cr} = 3 ± 1 g dm^{-3}, respectively) at which the surface tension attains a steady value of 33.0 ± 0.3 mN m^{-1}. The critical concentration defines the point at which the Gibbs monolayer is full and is used as an indirect indication of the concentration at

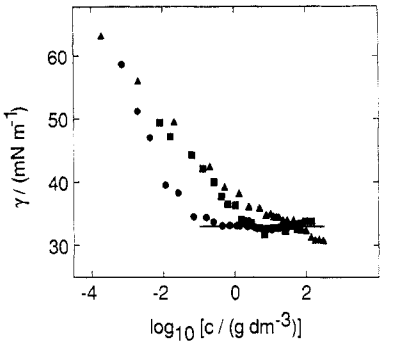

Figure 5. Surface tension (γ) versus copolymer concentration for aqueous solutions of block copolymers at 40 °C: (●) $E_{41}B_8$; (■) $E_{21}B_8E_{21}$; (▲) $B_4E_{40}B_4$.

which molecules first form associates in appreciable concentration, the argument being that adsorption at the air–water interface is favored over association until the monolayer is full. It may be noted that the effect is not in itself indicative of the formation of large micelles, as it is possible for the surface tension curve to become constant when association is limited to dimers and trimers.[21]

The corresponding plot for copolymer $B_4E_{40}B_4$ (see Figure 5) is less readily interpreted. Assuming a similar limiting value of the surface tension in the range $\gamma \approx 31$–33 mN m^{-1}, a value of log c_{cr} in the range 1.0–2.0 is indicated, i.e., $c_{cr} \approx 30$ g dm^{-3}. Confirmatory evidence for this treatment of the data is described later.

The slopes of the surface tension curves below c_{cr} are related to the excess concentration (Γ) of surfactant in the surface layer compared to the bulk through the Gibbs adsorption isotherm:

$$\Gamma = -(1/RT)(d\gamma/d \ln c) \quad (2)$$

Within the assumption that the concentration of solute in solution is negligible compared to its concentration in the surface layer, the values of Γ correspond to the areas per molecule in the surface monolayer

$$a = 1/\Gamma N_A \quad (3)$$

where N_A is Avogadro's constant. The values obtained from the results shown in Figure 5 are:

copolymer	$E_{41}B_8$	$E_{21}B_8E_{21}$	$B_4E_{40}B_4$
surface area (a/nm^2)	0.64	1.48	1.52

Values of a = 0.53–0.81 nm^2 were obtained previously[4] for E_mB_n copolymers in aqueous solution at 20 and 40 °C, and a value of a = 1.3 nm^2 was obtained[1] for copolymer $E_{58}B_{17}E_{58}$ in solution at 30 °C. The smaller molecular areas found for diblock copolymers adsorbed at the water–air interface, i.e., roughly half those found for comparable triblock copolymers, is an interesting result, with implications for adsorption of block copolymers at other interfaces.

Critical Temperatures from Static Light Scattering. Aqueous solutions of copolymer $E_{41}B_8$ were not investigated by this method, as the critical temperatures of solutions of sufficient concentration to allow reliable measurement of light scattering intensity (i.e., c > 1 g dm^{-3}) were at or below the lower temperature limit of the apparatus ($T \approx 15$ °C).

Curves of scattering intensity against temperature for solutions of copolymer $E_{21}B_8E_{21}$ were complicated by the low-temperature clouding referred to previously. Examples are shown in Figure 6. Clearing and clouding temperatures observed on cooling a range of solutions are shown in Figure 7. The intense scattering peaks associated

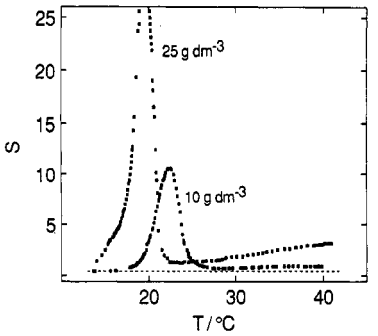

Figure 6. Light scattering intensity relative to that from benzene (S) versus temperature for aqueous solutions of copolymer $E_{21}B_8E_{21}$ with the concentrations indicated. The measurements were taken when cooling the solutions.

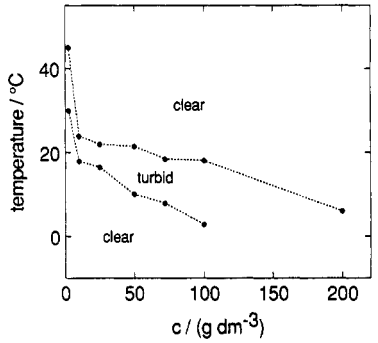

Figure 7. Clouding and clearing temperatures versus concentration of copolymer $E_{21}B_8E_{21}$ in aqueous solutions. The observations were made on cooling.

with the turbid solutions contrast with the much lower levels of scattering from associated species at higher temperatures. The low-T peak is assigned to phase separation, the sequence of events on raising the temperature being phase separation of the molecular solution followed closely by solubilization when the molecules associate, with corresponding reversed effects on cooling the solution. This explanation places the critical association temperature (T_{cr}) at or about the peak of the curve.

The effect has a parallel in the solubilization of crystalline, ionic surfactants at the Krafft point.[22] However, the details differ between crystalline and noncrystalline systems, particularly in the negative temperature derivative of solubility (liquid–liquid phase separation) in the present case. Turbidity below the critical association temperature was observed in studies of aqueous solutions of copolymer L64[10,21] and assigned to impurities on recognition that the effect could be removed by better purification[21] or by efficient filtration of the cloudy solutions.[10] In the present case the materials were adequately purified before the light scattering experiments were undertaken. Moreover, forcing cloudy solutions through 0.1-μm filters left them unchanged in scattering behavior, apart from the effect of dilution caused by unavoidable removal of material during filtration. While our experiments suggested an equilibrium effect, combining phase separation with association, it was noted that observations made on heating and cooling showed a hysteresis. Typically, the temperature at the maximum of the scattering peak on heating was a few degrees higher than than found on cooling. This effect was not investigated further.

Examples of scattering–temperature curves obtained for copolymer $B_4E_{40}B_4$ are shown in Figure 8. At the lowest concentration tested, 5 g dm^{-1}, the molecular solution was stable up to 60 °C and was cloudy at 61 °C. At concentrations of 10 g dm^{-1} and higher, a temperature at

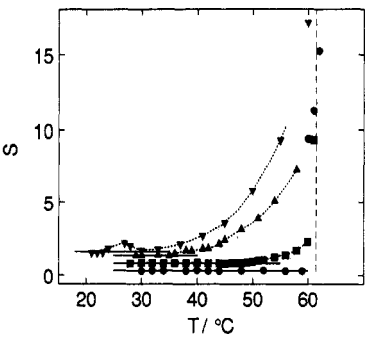

Figure 8. Light scattering intensity relative to that from benzene (S) versus temperature for aqueous solutions of copolymer $B_4E_{40}B_4$: (●) c = 5 g dm^{-3}; (■) c = 20 g dm^{-3}; (▲) c = 50 g dm^{-3}; (▼) c = 70 g dm^{-3}.

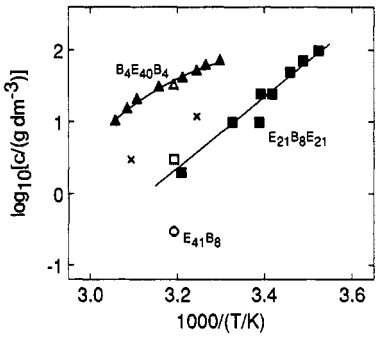

Figure 9. Critical conditions for association in aqueous solutions of block copolymer: logarithm of copolymer concentration versus inverse temperature for the copolymers indicated. Filled symbols represent results from the temperature dependence of light scattering, and open symbols represent results from the concentration dependence of surface tension. Crosses represent results from the concentration dependence of light scattering obtained for solutions of copolymer $E_{21}B_8E_{21}$: these were ignored in constructing the least-squares straight line (see text).

which a scattering curve left the "molecules" line was clearly identifiable (to ± 1 K) and was assigned to the critical association temperature (T_{cr}). At the highest concentration investigated (70 g dm^{-3}), slight clouding at or about T_{cr} indicated an effect similar to that described above for solutions of copolymer $E_{21}B_8E_{21}$. As seen in Figure 8, the intensity of scatter from the solutions of associated copolymer rose steadily in the temperature interval T_{cr}–60 °C, with no evidence of "micellar plateaux". Such plateaux are characteristic of closed associated[13,23] and were found for the solutions of copolymer $E_{21}B_8E_{21}$ at temperature above T_{cr} (see Figure 6). This observation is consistent with a wide distribution of particle sizes in solution, as indicated by dynamic light scattering (see previously).

It is useful to plot log c versus inverse critical association temperature: see Figure 9. Since the value of log c at T_{cr} corresponds to log c_{cr} at T, the results from surface tension can be entered on the same plot. As can be seen, they plot very well onto the results established by light scattering. The interpretation of this representation of the results is discussed later.

Molar Mass and Radius. As described previously, copolymer $E_{41}B_8$ in aqueous solution associated at low concentrations to form large particles ($r_h \approx 10$ nm), i.e., characteristic of micellization. Consequently, the determination of micellar molar mass and micellar radius from static light scattering was straighforward. Plots of the scattering function $c/(S-S_s)$ against c for copolymer $E_{41}B_8$ are shown in Figure 10: S is the intensity of light scattered from solution at 90° relative to the scattering from benzene, the S_s is the corresponding quantity for water. Within

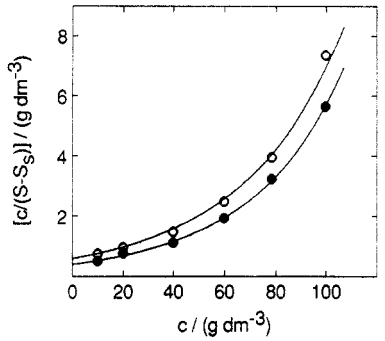

Figure 10. Light scattering function $c/(S - S_s)$ versus concentration (c) for aqueous solutions of copolymer $E_{41}B_8$ at (○) T = 20 °C and (●) T = 50 °C. S is the light scattering intensity relative to that from benzene, and S_s is the same quantity for pure solvent. The curves through the data points are constructed according to the Carnahan–Starling equation.

the concentration range covered, measurements of scattering intensities at 45° and 135° confirmed that the dissymmetry ($Z = S_{45}/S_{135}$) was approximately unity, i.e., that the scattering was from small particles. The pronounced curvature is a result of interparticle interference.

In keeping with early work on block copolymer micelles[24] and our own work on EB systems,[1-5] it was assumed that the micelles could be treated as hard spheres. Interparticle interference was accounted for writing the scattering equation in the form:

$$K^*c/(S - S_s) \sim 1/QM_w \tag{4}$$

where Q is the interparticle scattering factor (the intraparticle scattering factor being unity for small spheres), c is the concentration of micelles (in g dm^{-3}), and M_w is the mass-average molar mass of the micelles. As suggested by Vrij,[25] Q can be calculated from the Carnahan–Starling equation:[26]

$$1/Q = [(1 + 2\phi)^2 - \phi^2(4\phi - \phi^2)](1 - \phi)^{-4} \tag{5}$$

where ϕ is the volume fraction of equivalent thermodynamic uniform spheres, which can be calculated from the actual volume fraction of copolymer in micelles in the system by applying a volume swelling factor (δ_t = swollen volume relative to dry volume). The adjustable parameters are M_w and δ_t. This procedure is equivalent to taking the virial expansion out to its seventh term.

The refractive index increment determined for the present copolymers was 0.133 ± 0.002 cm^3 g^{-1} at 30 °C, which was in satisfactory agreement with values obtained previously[4] for aqueous solutions of comparable E_mB_n copolymers. The temperature derivative of dn/dc obtained previously[4] (-2×10^{-4} cm^3 g^{-1} K^{-1}) was used to derive values of K^* for the other temperatures considered. Concentrations were converted to a volume fraction basis assuming a density of dry polymer of $\rho \approx 1.07$ g cm^{-3} irrespective of temperature.

As can be seen in Figure 10, light scattering results for solutions of copolymer $E_{41}B_8$ at both 20 and 50 °C are well fitted by theory over the concentration range considered (c from 10 to 100 g dm^{-3}). Assuming a similar temperature dependence of the critical micelle concentration for solutions of copolymer $E_{41}B_8$ to that found previously[6] for related diblock copolymers (e.g., $E_{27}B_7$), critical micelle concentrations are expected to be *ca.* 3 g dm^{-3} at 20 °C and *ca.* 0.1 g dm^{-3} at 50 °C, i.e., well below the lower limit of concentration considered in Figure 10. Values of M_w and thermodynamic radius

$$r_t = (3\delta_t M_w/4\pi N_A \rho)^{1/3} \tag{6}$$

are listed in Table 2, as are association numbers of the micelles calculated from:

$$N_w = M_w(\text{micelle})/M_w(\text{molecule}) \tag{7}$$

where M_w(molecule) is listed in Table 1. Results for solutions at intermediate temperatures, not shown in Figure 10, are also included in Table 2. As expected, considering previous results and those presented above, values of M_w were found to increase with temperature, from 110 000 to 210 000 g mol^{-1} as T was increased from 20 to 50 °C, consistent with association numbers in the range 40–80. Micellar thermodynamic radii also increased with temperature, from 5.2 to 6.5 nm. Similar trends have been found previously[4] for aqueous solutions of E_mB_n copolymers.

Aqueous solutions of copolymers $E_{21}B_8E_{21}$ and $B_4E_{40}B_4$ had high values of c_{cr}: e.g., from surface tension at 40 °C, $c_{cr} \approx 3$ g dm^{-3} for $E_{21}B_8E_{21}$ and $c_{cr} \approx 30$ g dm^{-3} for $B_4E_{40}B_4$, compared with 0.3 g dm^{-3} for copolymer $E_{41}B_8$. Consequently, high temperatures and high concentrations were needed for these copolymers to associate. Indeed, results obtained for solutions of copolymer $B_4E_{40}B_4$ at 30 °C (not shown) confirmed the absence of association below c = 80 g cm^{-3} and, when extrapolated to c = 0, gave an intercept corresponding to M_w = 2300 ± 400 g mol^{-1}, i.e., corresponding to the molar mass of the unassociated copolymer molecules.

Plots illustrating association of copolymers $E_{21}B_8E_{21}$ and $B_4E_{40}B_4$ in solution at 50 °C are shown in Figure 11. The level of scattering expected for the unassociated copolymers is indicated on the diagram, as are the critical concentrations for the two copolymers in solution at 50 °C, as estimated from Figure 9. The high values of $c/(S - S_s)$ at low-to-moderate concentrations result from low extents of association and are consistent with high critical concentrations. In the case of copolymer $E_{21}B_8E_{21}$, the evidence is that association predominates in the system at high concentration, whereas it is difficult to assign a region in which association predominates for copolymer $B_4E_{40}B_4$.

In order to calculate the masses and sizes of the associates in the presence of unassociated copolymer, it was assumed that the concentration of associated species could be approximated by deducting c_{cr} from the total copolymer concentration. Accordingly, the scattering function $(c - c_{cr})/(S - S_s)$ is plotted against $(c - c_{cr})$ in Figure 12. For copolymer $E_{21}B_8E_{21}$, the values of c_{cr} chosen were the minimum needed to compensate for the upturn at low concentrations: c_{cr} = 12 and 3 g dm^{-3} at 35 and 50 °C, respectively, gave satisfactory results (see Figure 12). For copolymer $B_4E_{40}B_4$, values of c_{cr} = 16 and 8 g dm^{-3} at 50 and 60 °C were taken directly from Figure 9. The correction was insignificant for solutions of copolymer $E_{41}B_8$.

For copolymer $E_{21}B_8E_{21}$, the "corrected" plots shown in Figure 12 were fitted by the Carnahan–Starling equation, as described previously. The intercepts corresponded to M_w = 12 000 and 15 000 g mol^{-1}, i.e., different from the values of M_w = 10 000 and 17 000 g mol^{-1} obtained (with less precision) from the intercepts shown in Figure 11 but within the estimated experimental error of ±10%. The values of M_w and r_t obtained at the two temperatures are listed in Table 2. These results are securely obtained by the fitting procedure, but the interpretation of the values of the radii of the associates of copolymer $E_{21}B_8E_2$ is not

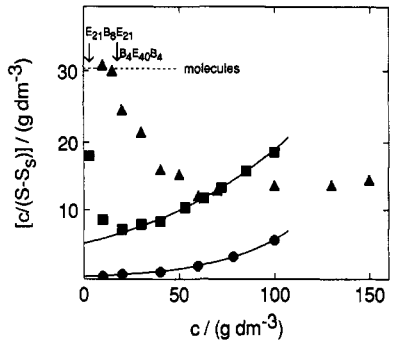

Figure 11. Light scattering function $c/(S - S_s)$ versus concentration (c) for aqueous solutions of copolymers at 50 °C: (●) $E_{41}B_8$; (■) $E_{21}B_8E_{21}$; (▲) $B_4E_{40}B_4$. S is the light scattering intensity relative to that from benzene and S_s is the same quantity for pure solvent. The arrows indicate the critical concentrations for association (estimated from Figure 9) for copolymers $E_{21}B_8E_{21}$ and $B_4E_{40}B_4$, as indicated. The curves through the data points for copolymers $E_{41}B_8$ and $E_{21}B_8E_{21}$ are constructed according to the Carnahan–Starling equation.

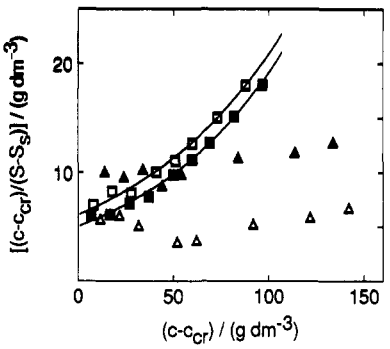

Figure 12. Light scattering function $(c - c_{cr})/(S - S_s)$ versus concentration minus the critical association concentration ($c - c_{cr}$) for aqueous solutions of block copolymers: $E_{21}B_8E_{21}$ at (□) T = 35 °C and (■) T = 50 °C; $B_4E_{40}B_4$ at (▲) T = 50 °C and (△) T = 60 °C. S is the light scattering intensity relative to that from benzene, and S_s is the same quantity for pure solvent. The curves through the data points for copolymer $E_{21}B_8E_{21}$ are constructed according to the Carnahan–Starling equation.

immediately obvious, since, in that case, very small associates ($N_w \leq 6$) were modeled as hard spheres. Nevertheless, it is clear that the overall pattern of behavior for copolymer $E_{21}B_8E_{21}$ is that of micellization *via* closed association, as found for copolymer $E_{41}B_8$. Compared with the results obtained for copolymer $E_{41}B_8$, the smaller values of M_w and r_t obtained for copolymer $E_{21}B_8E_{21}$ fit well to the pattern established by the dynamic light scattering measurements described previously.

The results for copolymer $B_4E_{40}B_4$ in solution at 50 and 60 °C do not fit the closed micellization pattern. Comparison with the results obtained for copolymer $E_{21}B_8E_{21}$ (see Figure 12) is most revealing. In the case of copolymer $B_4E_{40}B_4$, the scattering function $(c - c_{cr})/(S - S_s)$ is approximately independent of $c - c_{cr}$ over the concentration range studied. This is explicable if an increase in $c - c_{cr}$ is offset by an increase in the average molar mass of the associates, with a consequent increase in the value of $S - S_s$. In fact, for 50 °C the scattering function $(S - S_s)$ varies in value from a level consistent with trimers ($N_w \approx 3$) at low values of $c - c_{cr}$ to one considerably higher than that found for micelles of copolymer $E_{21}B_8E_{21}$ at high values of $c - c_{cr}$. This is behavior of the type expected for open association,[27] and in this respect the concentration dependence of static light scattering from solutions of copolymer $B_4E_{40}B_4$ is seen to be consistent with the results described above, from dynamic light scattering and from the temperature dependence of static light scattering. Correspondingly, the scattering from low-concentration solutions at 60 °C is consistent with $N_w \approx 7$, but with much higher values at higher concentrations. As a consequence of this behavior, characteristic values of the molar masses and radii of the associates cannot be derived from static light scattering for copolymer $B_4E_{40}B_4$, and none are included in Table 2.

Table 3. Critical Concentrations for the Association of Block Copolymers in Aqueous Solution[a]

		c_{cr}/(g dm^{-3})		
			light scattering	
copolymer	T/°C	surface tension	T_{cr}[a]	c_{cr}[b]
$E_{41}B_8$	40	0.3		
$E_{21}B_8E_{21}$	20		23	
	30		7	
	35			12
	40	3	2	
	50			3
$B_4E_{40}B_4$	40	≈30	35	
	50		16	
	60		8	

[a] From the temperature dependence of light scattering; see Figure 9. [b] From the concentration dependence of light scattering; see text.

The nature of the association of copolymer $B_4E_{40}B_4$, leading to large particles, was not further explored. We speculate that two processes may be involved: stepwise growth of associates at low concentrations and aggregation of the associates (micelles) at moderate concentrations, the strong interactions necessary for the latter process originating in the dynamic equilibration of copolymers between conformations with both end blocks in the same micelle and those with the two end blocks in different micelles. With regard to aggregation of micelles, a related but not identical model has been proposed by Tuzar *et al.*[28] for a micellar solution of an ABA block copolymer in a selective organic solvent for the A block.

The results of light scattering from solutions of copolymer $B_4E_{40}B_4$ at 60 °C carry an additional point of interest, in that they were carried out on solutions only a degree or so below the temperature assigned as the cloud point. Clouding directly attributable to phase separation of the molecular solution was detected for a solution of concentration 5 g dm^{-3} (see Figure 8), i.e., at a concentration well below the critical association concentration predicted for 60 °C (10 g dm^{-3}; see Figure 9). In fact the solutions of moderate to high concentration examined in the scattering experiments summarized in Figure 12 were visibly clouded. Evidence of the same effect was seen in the marked increase in scattering intensity with temperature observed for solutions of moderate concentration (50–70 g dm^{-3}; see Figure 8), which resulted in visibly clouded solutions at the highest temperatures. This clouding effect is not attributed to phase separation but rather to the formation of very large, stable associates.

Thermodynamics of Association. Critical association concentrations obtained and used in this work are summarized in Table 3 and plotted, together with results from the temperature dependence of light scattering, in Figure 9. The results are broadly consistent between the three methods, though those derived for copolymer $E_{21}B_8E_{21}$ from the concentration dependence of light scattering (crosses in Figure 9) show a systematic divergence from the other results. Accurate measurements of low light scattering intensities are needed for reliable determination of c_{cr} from the concentration dependence of light scattering, and the present experiments were not designed for that purpose. The critical temperature method requires only a judgement of the temperature at which the scattering

curve leaves the base line, and those results are judged most reliable.

If the association number (N) is single-valued (or the average of a narrow distribution of values), the association equilibrium can be simply written,

$$A = (1/N)A_N \qquad K = [A_N]^{1/N}/[A] \tag{8}$$

If the association number is large ($1/N \rightarrow 0$), then the equilibrium constant $K \rightarrow 1/[A]$ and, taking $[A]$ to be c_{cr}, the standard Gibbs energy and the enthalpy of association are given by:

$$\Delta_{assoc}G^\circ \approx RT \ln (c_{cr}) \tag{9}$$

$$\Delta_{assoc}H^\circ \approx R\{\mathrm{d} \ln (c_{cr})/\mathrm{d}(1/T)\} \tag{10}$$

The process refers to standard states of copolymer chains in an ideally dilute solution at unit concentration (1 mol dm^{-3}) and copolymer chains in the associated state.

In the case of copolymer $E_{21}B_8E_{21}$, the distribution of N is narrow, but the average value is small (N = 5–6; see Table 2). Numerical calculation showed that the error in using eq 10 under these circumstances was tolerable: i.e., *ca.* +10% in $\Delta_{assoc}H^\circ$.[29] The calculation was carried out as follows. For an advancement α of equilibrium (8),

$$K = [(\alpha/N\beta)^{1/N}\beta/(1-\alpha)](1/c)^{1-1/N} \tag{11}$$

where c = total concentration in mol dm^{-3} and $\beta = 1 - \alpha + (\alpha/N)$. Equation 11 reverts to $K = 1/c$ as $\alpha \rightarrow 0$ and $N \rightarrow \infty$. Values of K at various of T were calculated for small values of α and $c = c_{cr}$, and the value of $\Delta_{assoc}H^\circ$ obtained therefrom was compared with that calculated from eq 9, i.e., from $K \approx 1/c_{cr}$. The calculated error was insensitive to the choice of α.

The approximate value of $\Delta_{assoc}H^\circ$ calculated directly from the slope of the straight line drawn through the data points for copolymer $E_{21}B_8E_{21}$ (see Figure 9) was +95 kJ mol^{-1}. This value is in fair agreement with that obtained by the same method for diblock copolymers $E_{28}B_5$ and $E_{27}B_7$, i.e., +80 kJ mol^{-1}.

The corresponding experimental results for copolymer $B_4E_{40}B_4$ lie on a curve: see Figure 9. Extraction of meaningful thermodynamic parameters from these results would require a dependent stepwise growth of associates. Several association models are available, covering a range of cooperative to anticooperative associations,[30] and their application to the present results for copolymer $B_4E_{40}B_4$ is under consideration.

Gelation. Within the concentration and temperature ranges investigated (i.e., c up to 700 g kg^{-1}, T from 0 to 70 °C), solutions of copolymers $E_{21}B_8E_{21}$ and $B_4E_{40}B_4$ did not gel. Concentrated solutions of copolymer $E_{41}B_8$ gelled, as illustrated in Figure 13 where comparison is made with results obtained[6] for copolymer $E_{30}B_8$.

Limited separation of water from the gel (syneresis) was observed on heating the gel toward the high-temperature limit of the gel region. Otherwise the systems were homogeneous, both inside and outside the gel–sol boundary. Water was exuded as a thin surface film. The effect is ascribed to an elastic response of the gel toward thermal expansion.

If, as has been shown directly for other systems,[1,15] gelation results from close packing of micelles acting effectively as hard spheres, then the critical gelation concentration (c_{gel} in g dm^{-3}) is given by:

$$c_{gel} = (2^{1/2}/8r_{hs}^3)(10^{24}M/N_A) = 0.292M/r_{hs}^3 \tag{12}$$

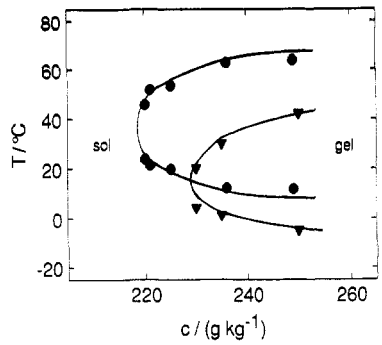

Figure 13. Gel–sol boundaries for solutions of block copolymers (●) $E_{41}B_8$ and (▼) $E_{30}B_8$. Concentration in grams of copolymer per kilogram of solution.

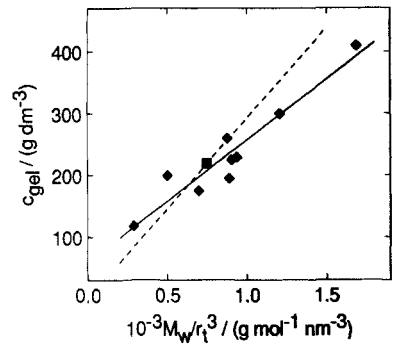

Figure 14. Critical concentration for gel formation (c_{gel}) versus M_w/r_t^3 for aqueous micellar solutions of oxyethylene/oxybutylene block copolymers: (■) copolymer $E_{41}B_8$ from present work; (●) diblock and triblock copolymers from previous work: see ref 6. The full line is calculated from eq 13, and the dashed line, from eq 11.

where r_{hs} is the equivalent hard-sphere radius in nm and M is the molar micellar mass in g mol^{-1}. Equation 12 can be applied to the present case *via* the molecular weights (M_w) and thermodynamic radii (r_t) determined by static light scattering: see Table 2. Previous results[6] fit the approximate relationship

$$c_{gel} \approx 60 + 0.20(M_w/r_t^3) \tag{13}$$

The relationship of the present to the previous results is shown in Figure 14, in which eqs 12 and 13 are also plotted. As can be seen, the hard-sphere equation 12 is a poor fit to the full range of available data, though it fits well enough in the present case.

At, e.g., 35 °C the concentrated solutions of both diblock copolymers, $E_{41}B_8$ and $E_{30}B_8$, are essentially wholly micellar. The lower concentration needed for gelation of a solution of copolymer $E_{41}B_8$, compared with that for a comparable solution of copolymer $E_{30}B_8$, is a consequence of its smaller value of M_w/r_t^3: 770 g mol^{-1} nm^{-3} for $E_{41}B_8$ compared with 900 g mol^{-1} nm^{-3} for $E_{30}B_8$. This value for copolymer $E_{30}B_8$ corresponds, *via* eq 13, to $c_{gel} \approx 240$ g kg^{-1}, i.e., very much as found (see Figure 13).

A similar calculation for copolymer $E_{21}B_8E_{21}$, based on the results in Table 2, predicts that solutions of this copolymer should gel at concentrations exceeding *ca.* 400 g kg^{-1}. This was not observed. Recent work[31] on a related triblock copolymer, $E_{20}B_{11}E_{20}$, has revealed a transition from a rigid-gel phase to a viscous phase in the concentration range 400–500 g kg^{-1}, presumably a consequence of a change in micellar shape. It is possible that copolymer $E_{21}B_8E_{21}$ attains its viscous phase without first forming a rigid-gel phase.

Acknowledgment. Prof. Provencher kindly provided copies of the CONTIN program for analysis of dynamic

light scattering data. Dr. R. H. Mobbs, Dr. F. Heatley, and Mr. K. Nixon gave valuable assistance with the preparation and characterization of the copolymers. Research studentships were provided by the Colloid Fund of the University of Manchester (N.-J.D.) and by SERC (R.J.B.). Interesting comments made by our reviewers stimulated certain points of discussion.

References and Notes

(1) Luo, Y.-Z.; Nicholas, C. V.; Attwood, D.; Collet, J. H.; Price, C.; Booth, C. *Colloid Polym. Sci.* **1992**, *270*, 1094.
(2) Nicholas, C. V.; Luo, Y.-Z.; Deng, N.-J.; Attwood, D.; Collett, J. H.; Price, C.; Booth, C. *Polymer* **1993**, *34*, 138.
(3) Luo, Y.-Z.; Nicholas, C. V.; Attwood, D.; Collett, J. H.; Price, C.; Booth, C.; Zhou, Z.-K.; Chu, B. *J. Chem. Soc., Faraday Trans.* **1993**, *89*, 539.
(4) Bedells, A. D.; Arafeh, R. M.; Yang, Z.; Attwood, D.; Heatley, F.; Padget, J. C.; Price, C.; Booth, C. *J. Chem. Soc., Faraday Trans.* **1993**, *89*, 1235.
(5) Bedells, A. D.; Arafeh, R. M.; Yang, Z.; Attwood, D.; Padget, J. C.; Price, C.; Booth, C. *J. Chem. Soc., Faraday Trans.* **1993**, *89*, 1243.
(6) Tanodekaew, S.; Deng, N.-J.; Smith, S.; Yang, Y.-W.; Attwood, D.; Booth, C. *J. Phys. Chem.* **1993**, *97*, 11847.
(7) Schmolka, I. R. *J. Biomed. Mater. Res.* **1972**, *6*, 571.
(8) Chen-Chow, P. C.; Frank, S. G. *Int. J. Pharm.* **1981**, *8*, 89.
(9) Collett, J. H.; Tait, C. J.; Attwood, D.; Sharma, H. L.; Smith, A. M. *Proc. Int. Symp. Control. Rel. Bioact. Mater.* **1985**, *12*, 28.
(10) Zhou, Z.-K.; Chu, B. *Macromolecules* **1988**, *21*, 2548.
(11) Wanka, G.; Hoffmann, H.; Ulbricht, W. *Colloid Polym. Sci.* **1990**, *268*, 101.
(12) Brown, W.; Schillen, K.; Almgren, M.; Hvidt, S.; Bahadur, P. *J. Phys. Chem.* **1991**, *95*, 1850.
(13) Yu, G.-E.; Deng, Y.-L.; Dalton, S.; Wang, Q.-G.; Attwood, D.; Price, C.; Booth, C. *J. Chem. Soc., Faraday Trans.* **1992**, *88*, 2537.
(14) Malmsten, M.; Lindman, B. *Macromolecules* **1992**, *25*, 5440.
(15) Mortenson, K. *Phys. Chem. Lett.* **1992**, *68*, 2340; *Macromolecules* **1993**, *26*, 805.
(16) Ding, J.-F.; Heatley, F.; Price, C.; Booth, C. *Eur. Polym. J.* **1991**, *27*, 895.
(17) Yang, L.; Bedells, A. D.; Attwood, D.; Booth, C. *J. Chem. Soc., Faraday Trans.* **1992**, *88*, 1447.
(18) Heatley, F.; Yu, G.-E.; Sun, W. B.; Pywell, E. J.; Mobbs, R. H.; Booth, C. *Eur. Polym. J.* **1990**, *26*, 583.
(19) Heatley, F.; Yang, Z., to be published.
(20) Provencher, S. W. *Makromol. Chem.* **1979**, *180*, 201.
(21) Reddy, N. K.; Fordham, P. J.; Attwood, D.; Booth, C. *J. Chem. Soc., Faraday Trans.* **1990**, *86*, 1569.
(22) Attwood, D.; Florence, A. T. *Surfactant Systems*; Chapman and Hall: London, 1983; p 45.
(23) Deng, Y.-L.; Ding, J.-F.; Stubbersfield, R. B.; Heatley, F.; Attwood, D.; Price, C.; Booth, C. *Polymer* **1992**, *33*, 1964.
(24) Brown, R. A.; Masters, A. J.; Price, C.; Yuan, X.-F. In *Comprehesive Polymer Science, Vol. 2*; Booth, C., Price, C., Eds.; Pergamon Press: Oxford, U.K., 1989, Chapter 6.
(25) Vrij, A. *J. Chem. Phys.* **1978**, *69*, 1742.
(26) Carnahan, N. F.; Starling, K. E. *J. Chem. Phys.* **1969**, *51*, 635.
(27) Elias, H. G. In *Light Scattering from Polymer Solutions*; Huglin, M. B., Ed.; Academic Press: London, 1972; Chapter 9.
(28) Tuzar, Z.; Konak, C.; Stepanek, P.; Plestil, J.; Kratochvil, P.; Prochazka, K. *Polymer* **1990**, *31*, 2118.
(29) This error was underestimated in ref 6.
(30) Attwood, D.; Florence, A. T. *Surfactant Systems*; Chapman and Hall: London, 1983; p 111.
(31) Barlow, R. J.; Yang, Y.-W.; Booth, C., to be published.